stacles to the establishment of *A. albopictus*; a large fraction of treeholes contain only *A. triseriatus* as potential competitors (*5*). Our results indicate that competition with the predominant species in treehole communities, *A. triseriatus*, will be insufficient to prevent the establishment of *A. albopictus*.

REFERENCES AND NOTES

1. D. Shroyer, *J. Am. Mosq. Control* **2**, 424 (1986).
2. D. Sprenger and T. Wuithiranyagool, *ibid.*, p. 217.
3. *Am. Mosq. Control Assoc. Newsl.* **16** (no. 3), 13 (1990); *ibid.* **16** (no. 2), p. 5; *ibid.* **15** (no. 1), 15 (1989).
4. W. Hawley, P. Reiter, R. Copeland, C. Pumpuni, G. Craig, *Science* **236**, 1114 (1987).
5. W. Bradshaw and C. Holzapfel, *Oecologia* **57**, 239 (1983); *ibid.* **74**, 507 (1988); R. Copeland and G. Craig, *Ann. Entmol. Soc. Am.* **83**, 1063 (1990).
6. W. Black, K. Rai, B. Turco, D. Arroyo, *J. Med. Entomol.* **26**, 260 (1989); C. Ho, A. Ewert, L. Chew, *ibid.*, p. 615.
7. *Aedes albopictus* and one *A. triseriatus* population were established by mosquitoes collected in New Orleans, LA. Additional *A. triseriatus* populations were established by females from central Massachusetts. A three-way analysis of variance of the interactions of Louisiana and Massachusetts *A. triseriatus* with *A. albopictus* reveal no statistically significant differences between *A. triseriatus* strains (T. Livdahl, unpublished data), and the results presented here combine the results of both strains.
8. After removing mosquito larvae, without removing detritus, fluid contents of ten treeholes and ten tires were pooled and homogenized with a canoe paddle during fluid disbursement.
9. T. Livdahl and G. Sugihara, *J. Anim. Ecol.* **53**, 573 (1984).
10. Some cohorts failed to produce adult females. In such cases, the cohort was pooled with emergence data from another cohort within the same experimental cells, with r' calculation based on the total number of individuals for the pooled cohorts.
11. R. Sokal and F. Rohlf, *Biometry* (Freeman, New York, 1981), pp. 795–799.
12. J. Hard, W. Bradshaw, D. Malarkey, *Oikos* **54**, 137 (1989).
13. E. Walker and R. Merritt, *Environ. Entomol.* **17**, 199 (1988).
14. E. Schreiber, C. Meek, M. Yates, *J. Am. Mosq. Control* **4**, 9 (1988).
15. G. O'Meara, "The spread of *Aedes albopictus* and *Aedes bahamensis* in Florida," paper presented at the 1990 Annual Meeting of the Entomological Society of America, New Orleans, 2 to 6 December 1990.
16. J. Peterson, H. Chapman, O. Willis, *Mosq. News* **29**, 134 (1969).

17. We thank J. Edgerly-Rooks, S. Gaimari, and J. Turner for technical assistance, O. Sholes, R. Bertin, and two anonymous reviewers for helpful suggestions, J. Freier for *A. albopictus* eggs, and NIH for financial support (R15AI27940 to T.P.L.).

21 January 1991; accepted 30 April 1990

Structural Features That Give Rise to the Unusual Stability of RNA Hairpins Containing GNRA Loops

HANS A. HEUS* AND ARTHUR PARDI†

The most frequently occurring RNA hairpins in 16*S* and 23*S* ribosomal RNA contain a tetranucleotide loop that has a GNRA consensus sequence. The solution structures of the GCAA and GAAA hairpins have been determined by nuclear magnetic resonance spectroscopy. Both loops contain an unusual G-A base pair between the first and last residue in the loop, a hydrogen bond between a G base and a phosphate, extensive base stacking, and a hydrogen bond between a sugar 2′-end OH and a base. These interactions explain the high stability of these hairpins and the sequence requirements for the variant and invariant nucleotides in the GNRA tetranucleotide loop family.

RNA HAIRPINS CONSISTING OF A double-stranded stem and a single-stranded loop are among the most common structural motifs in RNA. RNA hairpin loops have been viewed simply as a means for the RNA strand to fold back on itself, and it was thought that the sequence of the loop might not be very critical. However, recent phylogenetic and thermodynamic studies have revealed strong size and sequence dependencies for hairpin loops in RNA (*1*). In particular, hairpins containing a tetranucleotide loop seem to be very important. Phylogenetic studies show that in ribosomal RNAs (rRNAs) tetranucleotide loops comprise more than 55% of all loops, and more than 50% of all tetranucleotide loops have the consensus sequence GNRA (where N can be any nucleotide and R is either G or A) (*1*). The GNRA hairpin loops also occur with high frequency in catalytic, phage, and eukaryotic signal-recognition particle (SRP) RNAs (*2*). The solution structure of another frequently occurring RNA hairpin, which belongs to the UNCG family of tetranucleotide loops, has been reported (*3*).

RNA hairpins containing the GNRA loop sequence have been shown to be substantially more stable, with melting transition temperatures (T_m) more than 4°C higher than other less frequently occurring sequences (*4*). These thermodynamic and phylogenetic data led to the proposal that GNRA tetranucleotide loops may be evolutionarily selected because of their high stability, which allows them to serve as nucleation sites for proper folding of larger RNAs (*5*). In this report we identify the structural properties that give rise to the sequence requirements and high stability of hairpins containing GNRA loops.

The GCAA and GAAA loops were chosen for these nuclear magnetic resonance (NMR) studies because they are the most frequently occurring members of the GNRA family. The full sequences of the two hairpins are shown in Fig. 1 (*6*). Proton and ^{31}P resonances were assigned by standard two-dimensional (2-D) NMR techniques (*7*). Short (<4.5 Å) ^1H-^1H distances were identified by 2-D nuclear Overhauser effect (NOE) spectroscopy, and Fig. 2 shows a portion of the spectrum that was used to assign aromatic and sugar C-1′ proton resonances for the GCAA hairpin. Assignment

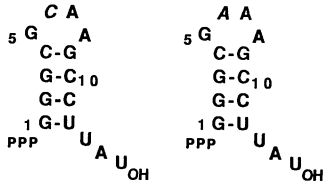

Fig. 1. The full sequences for the GCAA and GAAA RNA hairpins (*17*).

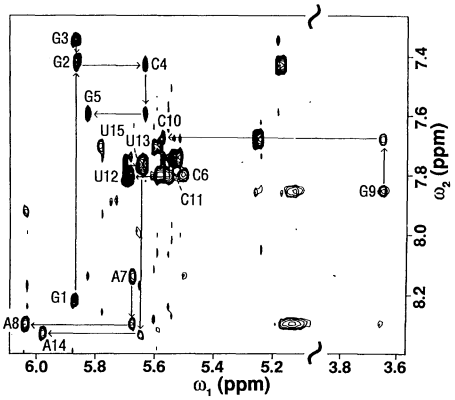

Fig. 2. A portion of the 2-D NOE spectrum of the GCAA hairpin in D_2O showing the aromatic H2/H8/H6 to sugar H1′/H5 region. This spectrum was taken with ~1.9 mM RNA hairpin in 100 mM NaCl, 10 mM sodium phosphate, pD = 6.8, at 25°C. Examples of sequential resonance assignment pathways involving H6/H8(n)-H1′9(n)-H6/H8(n+1) resonances are illustrated. Note the unusual upfield shift of the G9 H-1′.

Department of Chemistry and Biochemistry, University of Colorado at Boulder, Boulder, CO 80309.

*Present address: Department of Biophysical Chemistry, University of Nijmegen, Tournooiveld, 6525 ED Nijmegan, Netherlands.
†To whom correspondence should be addressed.

of the imino ^{1}H resonances was made from analysis of 1-D and 2-D proton NMR spectra in 90% H_2O (*8*). Qualitative inspection of the ^{1}H 2-D NOE spectra recorded in D_2O or 90% H_2O indicated an A-form type geometry for the duplex stems in both molecules (*8*). Analysis of the ^{1}H and ^{31}P chemical shifts and 2-D NOE data also indicated that the GCAA and GAAA hairpin loops had similar structures, so the discussion here will concentrate on the more frequently occurring (*1*) GCAA hairpin. All the ^{31}P resonances and all the nonexchangeable ^{1}H resonances (except the 3′ terminal sugar H-4′ and some of the H-5′ and H-5″ resonances) were assigned for this hairpin (*8*). The 3-D structures for the GCAA hairpin were determined by the use of ^{1}H-^{1}H distance constraints obtained from 2-D NOE spectra and backbone torsion angle and sugar pucker constraints derived from spin-spin coupling constants obtained from homo- and heteronuclear 2-D correlation spectroscopy experiments (*9*). The starting structures were generated by a distance geometry algorithm or by model-building on a graphics system and were then refined by constrained molecular dynamics calculations.

A stereoview for one of the refined structures of the tetranucleotide loop and three base pairs in the stem for the GCAA hairpin is shown in Fig. 3. The key features of the GCAA hairpin structure are summarized below and are shown schematically in Fig. 4A.

1) All nucleotides in the stem and loop have an anti-glycosidic angle conformation, as shown by the moderately sized intranucleotide H1′-H6/H8 NOEs.

2) The NMR structures also indicate the presence of an unusual G5-A8 base pair that is schematically shown in Fig. 4B. Two interbase hydrogen bonds are formed in this base pair: one from a G5 exocyclic amino proton to A8 N-7, and the other from an A8 exocyclic amino proton to G5 N-3. This base pairing is predicted from base geometries (*10*) and has been observed independently in a DNA duplex (*11*). Although we do not have direct NOE evidence for hydrogen bond formation, the structures generated from the observed distance and torsion-angle constraints are consistent with formation of this base pair. In our structures, one of the G5 amino protons is within standard hydrogen bonding distance (<2.0 Å) of the A8 N-7, but both A8 amino protons are greater than 2.9 Å from the G5 N-3. However, one of the A8 amino protons is also within hydrogen bonding distance (<2.0 Å) of the sugar 2′ oxygen on G5. This interaction may help to stabilize the formation of this G-A base pair. Additional support for this base pair was obtained from thermodynamic studies where the adenine bases in the GCAA hairpin were replaced by 7-deazaadenines (*12*). For the GCAA hairpin, the T_m is reduced by 4°C when the N-7, a potential hydrogen bond acceptor, is replaced by a C-7. As a control, thermodynamic studies were also performed on a UUUG hairpin with no adenines in the loop but with three standard Watson-Crick A-U base pairs in the stem. In this system, where the adenine N-7 is not involved in a hydrogen bond, there was no difference in T_m between the hairpin with adenines and the hairpin with 7-deazaadenines. These results are consistent with formation in the GCAA hairpin of a G-A base pair that is disrupted when the adenine N-7 is replaced by a C-7.

3) To accommodate this unusual G-A base pair, the helical twist for this base pair is small compared to a standard A- or B-form helix (*10*). This conformation for A8 is created by a G9 β torsion angle that is gauche instead of the normal trans. The constraint on the G9 β torsion angle was derived from the large H-5′ and H-5″ to ^{31}P coupling constants for this residue. The small helical twist brings A8 directly over the C-1′ proton on G9. In this conformation there is a large ring current effect of the A8 base on the G9 H-1′, which accounts for the unusual upfield chemical shift (shifted more than 1.5 ppm from the normal position) observed for this resonance.

4) Stacking of the bases in the loop ex-

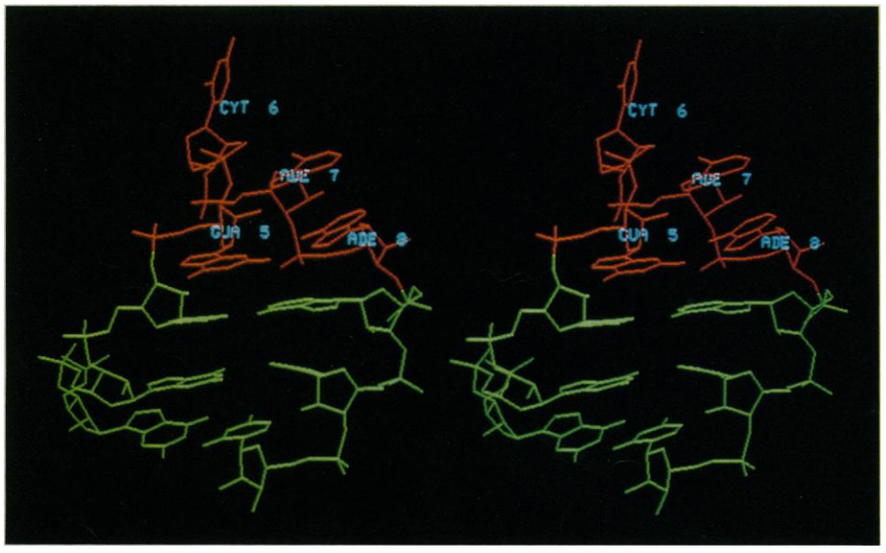

Fig. 3. Stereoview of the 3-D structure for G2 to C11 of the GCAA hairpin. The starting model for this structure was generated with the DSPACE (Hare Research, Woodinville, Washington) distance geometry program, and distance constraints were included so that the stem region formed an A-type helix. This structure was then energy-minimized and refined by constrained molecular dynamics with the program AMBER (*8*). A total of 38 NOE distance constraints and 11 β, γ, and ε backbone torsion angle constraints for nucleotides C4 through G9 were used in refining the structure. No torsion angle constraints were used for the α and ζ backbone torsion angles. N-type sugar puckers were included only for G5 and G9.

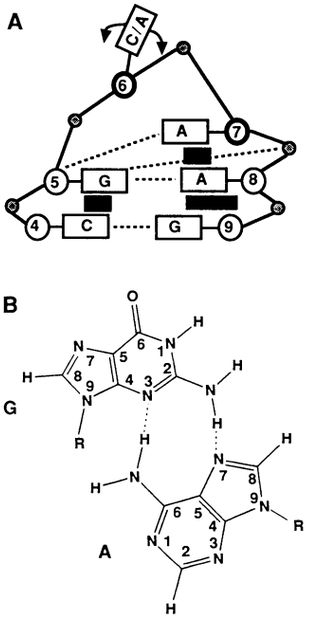

Fig. 4. (**A**) Schematic representation showing important structural features for the loops in the GCAA and GAAA hairpins (open circle, N-type sugar; boldface open circle, a mixture of N- and S-type sugars; box, base; stippled circle, phosphate; dotted line, hydrogen bond; and black box, stacking). In the GCAA hairpin, the C shows no interactions with other bases; however, in the GAAA hairpin, the second A in the loop stacks on the third A (*13*). (**B**) Schematic representation of G-A base pair with a configuration observed in the two RNA hairpins.

tends from the 3′ side, with A8 stacking on G9 and A7 stacking on A8, but C6 does not stack on G5 or A7. Instead, the sugar-phosphate backbone between G5 and C6 is extended, putting the C6 base on top of the hairpin loop. This conformation is supported by internucleotide H1′/H2′-H6/H8 NOEs observed between C6 and A7, and between A7 and A8, but not between G5 and C6. A similar pattern is observed for the GAAA hairpin (*8*).

5) A hydrogen bond is formed in the loop between one of the G5 amino protons and the A7pA8 phosphate oxygen. This interaction is indicated by the short distance from the amino proton to the oxygen in the NMR structures (<1.8 Å). In addition, the G5 imino proton exchanges relatively slowly with water protons and has a lifetime between that of the imino protons in the G-U base pair, which exchange more quickly, and that of the imino protons in the three G-C base pairs, which exchange more slowly (*13*). These data suggest that the G5 imino proton may not be freely accessible to solvent.

6) If we ignore the three 3′ terminal dangling nucleotides, all of the sugars occur predominantly in N-type (3′ endo) sugar pucker except for the C6 and A7 sugars, which on average have approximately 60% S-type (2′ endo) sugar pucker [a two-state model is assumed (*10*)]. These S-type sugar puckers tend to expand the sugar-phosphate backbone in the loop (*10*) and may be required to reverse the direction of the backbone.

7) The calculated structures also bring the G5 2′-end OH in proximity to the A7 N-7, which suggests a potential hydrogen bond between this N-7 and the hydroxyl proton.

The structural data presented here explain the sequence requirements of the GNRA tetranucleotide loop family. First, the base of the variable second nucleotide (N) in the loop is on the top of the hairpin and thus is not involved in any direct interaction. Second, the G at the first position must form a base pair with the A at the fourth position and must form a hydrogen bond with a phosphate residue. Finally, the third nucleotide in the loop must be a purine because its N-7 is proposed to be a hydrogen bond acceptor. A pyrimidine at this site cannot form this base-sugar hydrogen bond.

Another family of unusually stable RNA hairpins is represented by the UNCG tetranucleotide loops (*3*). As with the GNRA family, the UNCG family occurs frequently; it is the second most common hairpin loop in rRNAs (*1*). The GNRA and UNCG hairpin loops often seem to be evolutionarily interchangeable; that is, in one organism there is a GNRA loop closing a RNA helix, and, in an evolutionarily related organism, this RNA helix is closed by a UNCG loop (*1*). Comparison of the GNRA solution structure with that of a hairpin containing the UUCG tetranucleotide loop (*3*) reveals a number of intriguing similarities and differences between the structures of these two tetranucleotide loops.

1) In both structures there is an "extra" base pair between the first and last bases in the tetranucleotide loop, effectively leaving only a two-base loop; however, the nature of each of these base pairs is very different.

2) In both structures the variable second nucleotide is stacked on top of the loop and there are few (UUCG) or no (GCAA) short internucleotide proton-proton contacts between the first and second nucleotide.

3) Both structures contain a putative base-phosphate hydrogen bond, but the specific nucleotides involved are different in the two molecules.

4) The stacking of the bases in the two loops is different because the stacking extends primarily from the 5′ side in the UUCG loop, whereas it extends more from the 3′ side in the GCAA loop.

5) The middle two nucleotides in the UUCG loop have pure S-type sugar pucker, whereas in the GCAA loop these sugars are averages of S-type (60%) and N-type (40%) puckers. However, in both structures these S-type conformations extend the phosphate backbone to help bridge the ends of the stem duplex.

6) All of the nucleotides have an anti-glycosidic bond conformation in the GCAA loop, whereas the G in the UUCG loop has a syn conformation (which is required to accommodate its U-G base pair).

7) The base in position 3 in both loops is proposed to form a hydrogen bond with either the first sugar (in GCAA) or first phosphate (in UUCG) in the loop.

It has been suggested that the GNRA and UNGC tetranucleotide loop hairpins evolved independently and that they are evolutionarily interchangeable simply because of their unusual stability (*5*). The results presented here are consistent with this view, where the unusual stability observed for the GCAA hairpin is proposed to arise from additional specific hydrogen-bonding interactions among nucleotides in the loop. However, there are some examples of more specific functional roles for GNRA hairpin loops. The 3′ terminal GGAA hairpin of the small ribosomal subunit RNA has been implicated in initiation and fidelity of translation (*14*). In the eukaryotic SRP, a GAAA hairpin, essential for the SRP's function, binds specifically to the protein p19 (*15*). When base mutations are made in the GAAA loop that disrupt interactions predicted by our structural model, the SRP is functionally affected, whereas mutations that would be predicted to leave the loop structure unchanged appear to have no functional effect (*15*). The antimicrobial peptide ricin inactivates ribosomes by depurination in a specific hairpin loop in 28*S* rRNA (*16*). This hairpin could potentially form a GAGA tetranucleotide loop where the A in position 2 is depurinated in vivo. In our model this base is stacked on top of the hairpin loop and therefore is more accessible than other double- or single-stranded bases in the molecule, which could explain why it is the target for ricin. In a similar way, the structural model of the GCAA hairpin presented here should lead to an improved understanding of the biological roles of other GNRA tetranucleotide loops.

REFERENCES AND NOTES

1. C. R. Woese, R. R. Gutell, R. Gupta, H. F. Noller, *Microbiol. Rev.* **47**, 621 (1983); R. R. Gutell, B. Weiser, C. R. Woese, H. F. Noller, *Prog. Nucleic Acids Res. Mol. Biol.* **32**, 155 (1985); C. R. Woese, S. Winker, R. R. Gutell, *Proc. Natl. Acad. Sci. U.S.A.* **87**, 8467 (1990).
2. N. R. Pace, D. K. Smith, G. J. Olsen, B. D. James, *Gene* **82**, 65 (1989); R. B. Waring and R. W. Davies, *ibid.* **28**, 277 (1984); A. Jaquir and F. Michell, *Cell* **54**, 17 (1987); M. R. Adhin, J. Alblas, J. Van Duin, *Biochim. Biophys. Acta* **1050**, 110 (1990); M. A. Poritz, K. Strub, P. Walter, *Cell* **55**, 4 (1988).
3. C. Cheong, G. Varani, I. Tinoco, Jr., *Nature* **346**, 680 (1990).
4. J. Haney and O. C. Uhlenbeck, personal communication.
5. O. C. Uhlenbeck, *Nature* **346**, 613 (1990).
6. The sequence in the stem and the three single-stranded nucleotides attached to the 3′ end were chosen because extensive thermodynamic data have been obtained on these and a number of other hairpins with different tetranucleotide loop sequences (*4*).
7. K. Wüthrich, *NMR of Proteins and Nucleic Acids* (Wiley, New York, 1986), pp. 44–89.
8. H. A. Heus, P. Yip, A. Pardi, in preparation. The assignment procedure involved a combination of 2-D NOE, double quantum-filtered homonuclear correlated spectroscopy, total correlated spectroscopy, and ^{1}H-^{31}P heteronuclear correlated spectroscopy experiments (*7*).
9. The NOE distance constraints were designated as very weak (3 to 5 Å), weak (2.5 to 5 Å), moderate (2 to 4 Å), strong (1.8 to 3 Å), and very strong (1.8 to 2.5 Å). We calculated torsion angles from ^{1}H-^{1}H or ^{1}H-^{31}P J coupling constants using empirically determined Karplus equations [C. Altona, *Recl. Trav. Chim. Pays-Bas* **101**, 413 (1982); P. P. Lankhorst, C. A. G. Haasnoot, C. Erkelens, C. Altona, *J. Biomol. Struct. Dyn.* **1**, 1387 (1984)].
10. W. Saenger, *Principles of Nucleic Acids Structure* (Springer-Verlag, New York, 1984), pp. 55–282.
11. Y. Li, G. Zon, W. D. Wilson, *Proc. Natl. Acad. Sci. U.S.A.* **88**, 26 (1991).
12. RNA oligomers containing 7-deazaadenines were synthesized by incorporation of 7-deazaadenine 5′-triphosphate in the T7 RNA polymerase reactions (*17*). The sequence of the control RNA with no adenines in the loop and three A-U base pairs was GGGAUACUUUGGUAUCCA. Melting temperatures were determined in 10 mM sodium phosphate, 100 mM sodium chloride, 0.2 mM EDTA, pH 7, as described [D. R. Groebe and O. C. Uhlenbeck, *Biochemistry* **28**, 742 (1989)].
13. H. A. Heus and A. Pardi, unpublished data.
14. P. H. van Knippenberg in *Structure, Function and Genetics of Ribosomes*, B. Hardesty and G. Kramer,

Eds. (Springer-Verlag, New York, 1986), pp. 412–424.
15. V. Siegel and P. Walter, *Proc. Natl. Acad. Sci. U.S.A.* **85**, 1801 (1988); X. Liao, P. Brennwald, J. A. Wise, *ibid.* **86**, 4837 (1989).
16. Y. Endo, Y. L. Chan, A. Lin, K. Tsurugi, I. G. Wool, *J. Biol. Chem.* **263**, 7917 (1988).
17. The GCAA and GAAA hairpins were synthesized and purified as described [J. F. Milligan, D. R. Groebe, G. W. Witherell, O. C. Uhlenbeck, *Nucleic Acids Res.* **15**, 8783 (1987); H. A. Heus and A. Pardi, *J. Mol. Biol.* **217**, 113 (1991)] and dialyzed in 10 mM sodium phosphate, 100 mM sodium chloride, 0.2 mM EDTA, pH 7.0.
18. We thank O. C. Uhlenbeck for numerous discussions, F. Jucker for purification of the GCAA hairpin, M. Rance for collection of several of the NMR spectra, P. Yip for structure calculations, and L. Moon-McDermott for preparation of some of the 7-deazaadenine RNA oligomers. Supported by NIH grants AI 27026 and AI 30726. The NMR spectrometer was purchased with partial support from NIH grant RR03283. We also thank the W. M. Keck Foundation for support of RNA science at the University of Colorado at Boulder. This report is dedicated to the memory of Peter (Piet) H. Van Knippenberg, who devoted much of his career to the study of a member of the GNRA family, the GGAA hairpin loop.

22 January 1991; accepted 26 April 1991

Organizer-Specific Homeobox Genes in *Xenopus laevis* Embryos

BRUCE BLUMBERG,* CHRISTOPHER V. E. WRIGHT,† EDDY M. DE ROBERTIS, KEN W. Y. CHO

The dorsal blastopore lip of the early *Xenopus laevis* gastrula can organize a complete secondary body axis when transplanted to another embryo. A search for potential gene regulatory components specifically expressed in the organizer was undertaken that resulted in the identification of four types of complementary DNAs from homeobox-containing genes that fulfill this criterion. The most abundant of these encodes a DNA-binding specificity similar to that of the *Drosophila melanogaster* anterior morphogen *bicoid*. The other three are also homologous to developmentally significant *Drosophila* genes. These four genes may participate in the regulation of the developmental potential of the organizer.

THE DORSAL BLASTOPORE LIP FROM an early salamander gastrula, when implanted into the ventral side of a recipient gastrula, can organize the formation of a secondary body axis consisting of both host and graft-derived tissue (*1*). The dorsal blastopore lip was called the "organizer" to reflect its ability to recruit or organize host cells to form a secondary axis with appropriate anterior-posterior and dorsal-ventral polarity. The anterior-posterior extent of the secondary axis induced by the transplanted dorsal lips differed as gastrulation proceeded; dorsal lips from early gastrulae could induce nearly complete axes including heads, whereas dorsal lips from late gastrulae induced axes consisting of trunk and tail (*2*). The biochemical basis of the organizer phenomenon has, however, remained elusive, despite intensive investigation (*3*).

Experiments have shown that peptide growth factors related to transforming growth factor–β (TGFβ, XTC-MIF, activin) and basic fibroblast growth factor can induce mesoderm formation in uncommitted ectoderm and even confer organizer activity on treated ectoderm in transplantation experiments (*4*). Activin protein can organize body axis in uncommitted ectoderm and activin mRNA, injected into a single vegetal blastomere, can organize a secondary body axis (*5*). Although it is not known whether any of these molecules is a natural inducer in vivo, they are believed to be, or be related to, the actual molecules involved in mesoderm induction. The exact relation between mesoderm induction and the organizer phenomenon is not clear at present. However, these growth factors have been shown to influence the expression of several position-specific homeobox genes (*6*). Therefore, it has been postulated that mesoderm-inducing growth factors may provide positional information along the anterior-posterior axis by the regulation of the expression of homeobox genes (*6*).

Although single growth factors may induce a variety of mesodermal structures and even confer organizer-like activity on uncommitted ectoderm or microinjected blastomeres, the organizer's actual mode of action is likely to involve a number of molecules that jointly provide the spectrum of activities necessary for the induction of a body axis. That localized positional information exists in the organizer is indicated by experiments in which the salamander dorsal lip was divided into a number of fragments and cultured separately. The types of tissues formed by each fragment depended on its original location along the longitudinal axis in the dorsal lip (*7*). The quantity of organizer tissue in a *Xenopus laevis* embryo is directly proportional to the extent of anterior development (*8*). Thus, it can be inferred that the inductive potential of the organizer is dependent on both regional specialization in, and the overall size of, the dorsal blastopore lip.

We investigated the molecular basis of the organizer by isolating mRNA from excised dorsal lips [at stage (st) 10.25 gastrula when the dorsal lips are capable of inducing a complete secondary axis] (Fig. 1A). We then constructed a cDNA library from this mRNA, which is presumably enriched in molecules encoding proteins that provide positional information specific for the organizer, and screened for molecules that are likely to be involved in conferring organizer activity. As a first step in understanding what underlies regional specialization in the organizer, we decided to study a well-characterized family of genes known to be developmentally significant—those containing a homeobox. The homeobox is a DNA se-

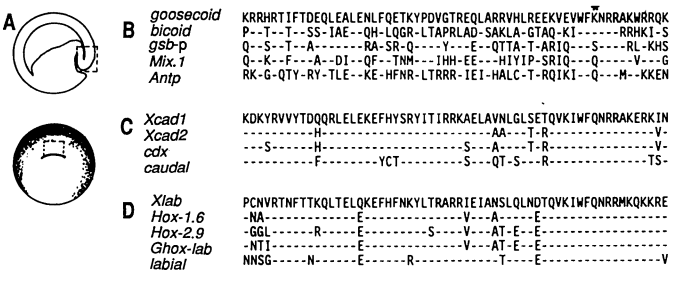

Fig. 1. Identification of the *Xenopus* organizer-specific homeobox. (**A**) Diagrammatic representation of the area used in the construction of the dorsal lip library. Dashed area indicates the extent of the dissected area used in the construction of the library. (Top) Cross-sectional view of the st 10.25 gastrula used; (bottom) external view of the same gastrula shown in (top). (**B** through **D**) Dorsal lip homeobox sequences (*29*). Asterisk indicates conserved Glu residue explained in text. Except where indicated, homeobox sequences used for comparison were derived from Scott and co-workers (*11*). (B) The relations among the products of *goosecoid* and related genes: *Mix.1* (*15*), *gooseberry*-proximal, *bicoid*, and *Antennapedia*. (C) The relations among the products of *Xcad1*, *Xcad2*, and the related genes *caudal* and *cdx* (*18*). (D) The products of *Xlab* and the related genes *Hox-1.6*, *Hox-2.9* (*37*), *labial*, and *GHox-lab* (*19*).

Department of Biological Chemistry, University of California, Los Angeles, CA 90024.

*To whom correspondence should be addressed.
†Present address: Department of Cell Biology, Vanderbilt University Medical School, Nashville, TN 37232.